Protection of Coastal Infrastructure under Rising Flood Risk

Megan J. Lickley, Ning Lin and Henry D. Jacoby

GLOBAL CHANGE

MIT JOINT PROGRAM ON THE
SCIENCE AND POLICY
of GLOBAL CHANGE

The MIT Joint Program on the Science and Policy of Global Change is an organization for research, independent policy analysis, and public education in global environmental change. It seeks to provide leadership in understanding scientific, economic, and ecological aspects of this difficult issue, and combining them into policy assessments that serve the needs of ongoing national and international discussions. To this end, the Program brings together an interdisciplinary group from two established research centers at MIT: the Center for Global Change Science (CGCS) and the Center for Energy and Environmental Policy Research (CEEPR). These two centers bridge many key areas of the needed intellectual work, and additional essential areas are covered by other MIT departments, by collaboration with the Ecosystems Center of the Marine Biology Laboratory (MBL) at Woods Hole, and by short- and long-term visitors to the Program. The Program involves sponsorship and active participation by industry, government, and non-profit organizations.

To inform processes of policy development and implementation, climate change research needs to focus on improving the prediction of those variables that are most relevant to economic, social, and environmental effects. In turn, the greenhouse gas and atmospheric aerosol assumptions underlying climate analysis need to be related to the economic, technological, and political forces that drive emissions, and to the results of international agreements and mitigation. Further, assessments of possible societal and ecosystem impacts, and analysis of mitigation strategies, need to be based on realistic evaluation of the uncertainties of climate science.

This report is one of a series intended to communicate research results and improve public understanding of climate issues, thereby contributing to informed debate about the climate issue, the uncertainties, and the economic and social implications of policy alternatives. Titles in the Report Series to date are listed on the inside back cover.

Ronald G. Prinn and John M. Reilly
Program Co-Directors

Protection of Coastal Infrastructure under Rising Flood Risk

Megan J. Lickley[*†], Ning Lin[**] and Henry D. Jacoby[*]

Abstract

The 2005 hurricane season was particularly damaging to the United States, contributing to significant losses to energy infrastructure—much of it the result of flooding from storm surge during hurricanes Katrina and Rita. In 2012, Hurricane Sandy devastated New York City and Northern New Jersey. Research suggests that these events are not isolated, but rather foreshadow a risk that is to continue and likely increase with a changing climate. Extensive energy infrastructure is located along the U.S. Atlantic and Gulf coasts, and these facilities are exposed to an increasing risk of flooding. We study the combined impacts of anticipated sea level rise, hurricane activity and subsidence on energy infrastructure with a first application to Galveston Bay. Using future climate conditions as projected by four different Global Circulation Models (GCMs), we model the change in hurricane activity from present day climate conditions in response to a climate projected in 2100 under the IPCC A1B emissions scenario. We apply the results from hurricane runs from each model to the SLOSH model to investigate the projected change in frequency and distribution of surge heights across climates. Further, we incorporate uncertainty surrounding the magnitude of sea level rise and subsidence, resulting in more detailed projections of risk levels for energy infrastructure over the next century. Applying this model of changing risk exposure, we apply a dynamic programming cost-benefit analysis to the adaptation decision.

Contents

1. RESPONDING TO A CHANGING CLIMATE

1.1 The Need for Improved Decision Support

Much of U.S. energy infrastructure is located on its coasts, and in recent years major hurricanes have affected substantial portions of the nation's energy system. For example,

---

[*] Joint Program on the Science and Policy of Global Change, Massachusetts Institute of Technology, Cambridge, MA.

[**] Earth, Atmospheric and Planetary Sciences, Massachusetts Institute of Technology; Department of Civil and Environmental Engineering, Princeton University, Princeton, NJ.

[†] Corresponding author (Email: mlickley@mit.edu)

Hurricane Katrina in August of 2005, followed by Hurricane Rita in September, delivered the "world's first integrated energy shock" (Yergin, 2006) as they disrupted oil, natural gas, and electric power generation, halting a quarter of U.S. oil production, one fifth of U.S. refining capacity and flooding several power generation plants. And in 2012, hurricane Sandy flooded extensive areas of New York City and Northern New Jersey. A large portion of the damage in these cases was the result of flooding from storm surge.

In coming decades the risks of coastal damage are projected to increase. Climate change brings increasing sea surface temperature, the engine of tropical storms, allowing them to grow in intensity and destructive power (Emanuel, 2005). Rising atmospheric and ocean temperatures also are causing sea level rise, through thermal expansion of the oceans and melting of mountain glaciers and continental ice sheets. Further contributing to flood risk in some areas is subsidence, by natural geological process or as stimulated by the removal of subsurface water and fossil fuels. All these processes are subject to uncertainty, and thus public and private officials responsible for these facilities face complex decisions about if, when, and how to take protective measures.

The main source of information about flood risk in the U.S. is the Federal Energy Management Agency (FEMA), which develops maps of 100- and 500-year flood risk (FEMA). It is a massive effort, covering the whole country, and the analysis of coastal flood risk includes elaborate statistical analysis of storm surge. FEMA mapping is the basis of the Federal Flood Insurance Program, and is the most important source of information for current public and private decisions about investment, building regulations, zoning, etc. Because of the focus on current facility and land-use decisions and insurance the FEMA analysis is based on current climatology and does not provide information about changing risk in future decades.

Here we address what type of information would be useful as support for adaptation decisions over time and how it might be developed. In addition, we explore how risk information might be applied as an input to support current decisions considering the fact that adaptation is a sequential process. What is economic to do now is dependent on the opportunity for action later, which leads conveniently to the formation of decision support for adaptation in a dynamic programming framework.

2. A SAMPLE ANALYSIS

A complete analysis of risk to coastal energy infrastructure would need to consider a variety of types of facilities, different forms of damage (wind, flooding from rainfall), change in risks across locations, various emissions scenarios and multiple projections of climate response. To demonstrate a possible approach to the development of such studies, we narrow the scope of the analysis to the risk of flooding from sea level rise, storm surge and subsidence of a sample facility in Galveston Bay. The Galveston area has seen extremely destructive hurricanes, the deadliest of which in 1900 destroyed the city of Galveston and killed upwards of 6000 people. The 20th century saw adaptation efforts, and still in 2008 Hurricane Ike caused nearly $30 billion in damage to the City.

Galveston Bay is an active seaport populated with oil refineries, a number of natural gas and coal power plants and components of the U.S. Strategic Petroleum Reserve. A sample of the

largest facilities is shown in **Figure 1**. The land around Galveston Bay is low lying, and much of this energy infrastructure sits 5 to15 feet above mean sea level. Further, the area is experiencing severe subsidence (Galloway *et al.*, 1999); some regions have sunk as much as ten feet over the past century, thought to be mainly due to the removal of ground-water and the production of oil and natural gas.

Two other points in Figure 1 are of special note. The center of the 100 km circle is the reference point for aspects of the hurricane analysis below. And Point A is the location of the particular facility that is carried through the analysis of changing flood risk and adaptation decisions.
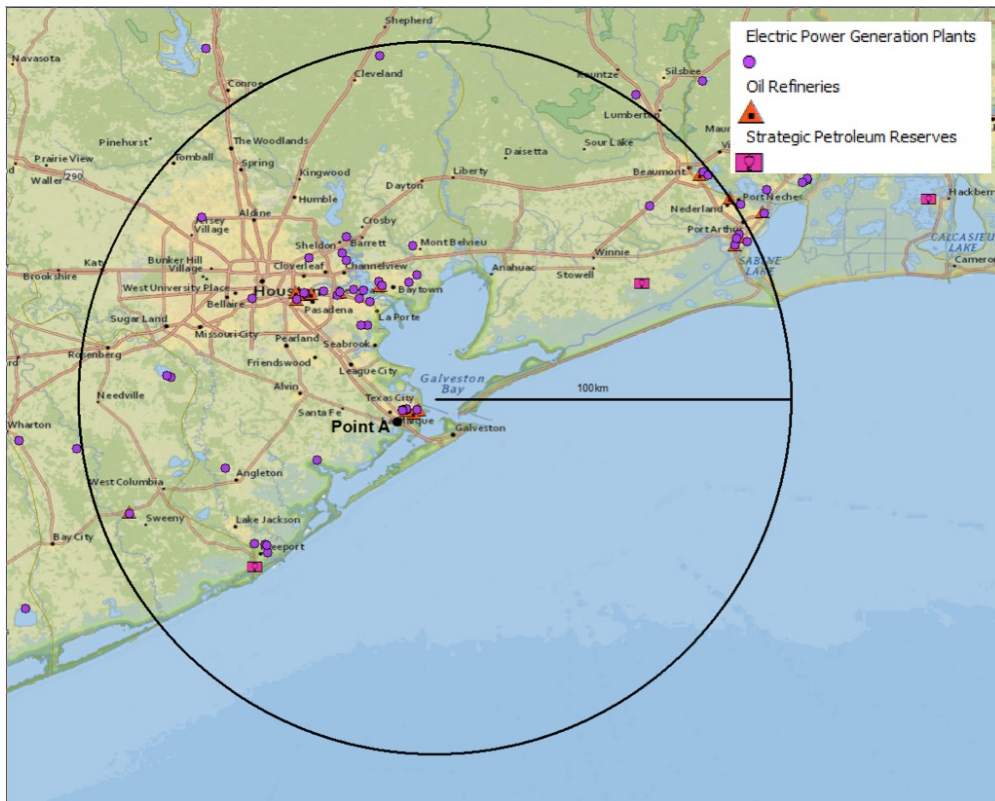

Figure 1. Electric generating units in Galveston region with 100 km filter for hurricane tracks, centered in Galveston Bay.

For this case study we consider conditions under just one emissions scenario, A1B, as defined by the IPCC and applied in its Fourth Assessment Report or AR4 (Solomon *et al.*, 2007). Results from 18 Atmosphere-Ocean General Circulation Models (AOGCMs) reviewed in the AR4 project that temperature change over this century will be somewhere between 1.7 and 4.4^{o}C under this scenario, and that sea level rise will be between 0.21 and 0.48 m. We employ four of the 18 archived model scenarios in the analysis of hurricane arrivals, and an overlapping set of six provide inputs to estimates of one of the components of sea level rise.

All the analysis that follows therefore is conditional on this A1B scenario. Also, the results of

each AOGCM are conditional on just the particular run of the model included in the AR4 archive and do not consider any uncertainty in the model itself or its natural variability (Deser *et al.*).

3. PHYSICAL ANALYSIS OF FLOOD RISK

For analysis of adaptation to changing flood risk we first need a description of the annual flood risk and how it is projected to change over time—in this study as influenced by the change between the climate in 1981–2000 and that projected for 2080–2100[1]. Two climate-related influences need to be considered: storm surge and sea level rise. To estimate the risk at a particular geographical point account also needs to be taken of land subsidence and astronomical tides. These four processes are then combined to produce the estimate of flood risk.

The estimation of storm surge risk begins with the generation of the tracks and wind fields of a large set of synthetic hurricanes, driven by climatic conditions represented in the AOGCMs used, passing through Galveston Bay. Statistics are estimated, first for the wind conditions of the sample of storms and, after passing through a model of storm surge, for the associated surge level at the point of interest. Statistics for the storms that do arrive are then combined with analysis of the frequency of arrival to yield estimates of the annual probability of storm surge at different levels above mean sea level. These results are combined with an assumption about tidal conditions at the time of storm arrival.

Sea level rise is considered in two parts: the contribution of thermal expansion of the ocean and the melting of glaciers and small ice caps, and the potential loss from the continental ice sheets of Greenland and Antarctica. Finally, since it is the relative sea level at the facility that matters, contribution to future risk of subsidence is added. The ultimate result is the probability that the facility will be flooded in 2000 and in 2100, which can be interpolated to the decades in between to support analysis (in Section 4) of when flood protection should be added to a facility at Point A in Figure 1, and at what level.

3.1 Storm and Storm Surge

3.1.1 Storm Generation

Each year approximately ten tropical storms develop in the North Atlantic, Caribbean, and Gulf of Mexico. On average six of these develop into hurricanes, of which only one or two make landfall in the U.S. (NOAA). Because the record of hurricane activity is so limited, analysis of flood risk cannot be based strictly on historical data. We apply a statistical-deterministic hurricane model developed by Emanuel *et al.* (2006) and Emanuel *et al.* (2008) to generate a large number of synthetic storms and a hydrodynamic model to generate the storm surges induced by these storms (Lin *et al.*, 2010) and (Lin *et al.*, 2012). The synthetic storms are simulated under the 2000 climate and projected 2100 climate to see how changes in climate alters storm and storm surge risk. Briefly summarized, the procedure involves three steps:

---

[1] These multi-year periods are needed to damp out year-to-year variability. To simplify the presentation we refer to these periods as 2000 and 2100 respectively.

- **Genesis by Random Seeding.** Storm seeds are distributed randomly throughout the Atlantic Basin as warm-core vortices with minimum peak winds. Most quickly decay.

- **Development of Storm Tracks.** A model of storm movements tracks the evolution of surviving storms in time and space based on winds and other factors that influence storm development. Tracks that pass though a filter defined as within a 100 km radius of the reference point in Galveston Bay shown in Figure 1 (29.3^{o}N, 94.5^{o}W) are kept and the rest discarded.

- **Storm Intensity.** For tracks that pass through the filter, the Coupled Hurricane Intensity Prediction System (CHIPS) (Emanuel *et al.*, 2004) is run to determine the intensity of the storm. At this point only tracks having the maximum wind speed greater than 34 mph within the filter are kept.

Figure 2 shows a sample of 50 of the resulting tracks.
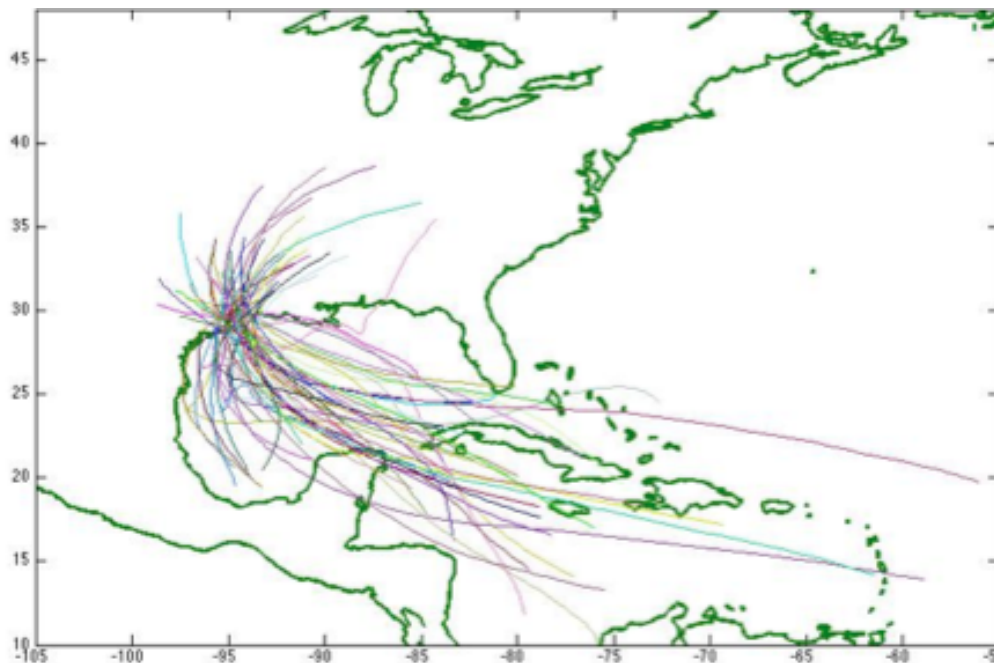
Figure 2. 50 of the storm tracks used in the analysis, passing through filter centered at Galveston.

This procedure is applied under conditions simulated in each climate model for current conditions (2000) and for 2100 based on the version of the A1B emissions scenario as recorded in the World Climate Research Program (WCRP) third Climate Model Intercomparison Project (CMIP3) multimodel data set (Meehl *et al.*, 2007). The four models used are listed in **Table 1**. For each of the four climate models and for each of the two climate conditions, we generate 3000 storms for the study area. The output of each storm track provides information on a 2-hour time step including storm location, radius of maximum wind, maximum wind speed and storm center pressure.

5

Table 1. Four AOGCMs. Temperature projections based on the A1B emissions scenario.

Model Name	Institute	Predicted Temperature Increase by 2100 in ^{o}C
CNRM-CM3	Le Centre National de Recherches Meteorologiges, Meteo-France	2.9
ECHAM	Max Planck Institution	3.4
GFDL-CM2.0	NOAA Geophysical Fluid Dynamics Laboratory	2.7
MIROC 3.2	CCSR/NIES/FRCGC, Japan	4.5

Wind speed provides one measure of storm intensity, and the 3000 tracks through the filter provide a basis for constructing a distribution of storm intensities at Galveston Bay, conditional on a storm arriving that meets the minimum wind speed criterion above. As an example, **Figure 3** shows the cumulative distribution of the storm maximum wind speed when the storm is at its closest point to the reference location in the Bay. Included are results for the year 2000 for each of the four climate models. These distributions then differ between 2000 and 2100 and the results for windspeed for all four models are presented in **Figure 4**. The biggest difference in windspeed is seen most clearly in the GFDL model where the probability of an arriving storm having a maximum wind speed greater than 100 mph increases from 0.2 in 2000 to 0.3 in 2100. The other models produce a smaller change even though they project greater temperature increases. This difference among models is not surprising since neither atmospheric nor sea surface temperatures alone are enough to determine the intensity of tropical storms. Other environmental factors including vertical wind shear, temperature distribution of the upper ocean, and humidity may all contribute to a storm's intensity. [2]

3.1.2 Surge Simulation

As hurricane intensity increases there is an anticipation of increased storm surge, leading to a greater potential for flooding. Storm surge occurs when sustained wind forces act on a body of water, forcing coastal shallow water up onto the shore. The height of the surge is determined by a number of factors including storm track, intensity and size, as well as coastal geometry and bathymetry. Given all of these factors, it is difficult to make straightforward calculations relating storm intensity to storm surge. There are attempts to generalize the relationship between storm intensity and storm destructive potential (including the surge effect), like that described by the Saffir-Simpson scale, but since maximum wind speed alone does not determine the height of the surge, we apply the SLOSH model (Sea, Lake and Overland Surges from Hurricane) developed by the U.S. National Oceanic an Atmospheric Administration (Jelesnianski *et al.*, 1992) for a more detailed storm surge analysis. Results from each hurricane run are input to this model of

---

[2] Note that the exceedance probability is 1 – cumulative probability. These plots are conditional on storm arrival and do not show the change in their frequency (discussed later).
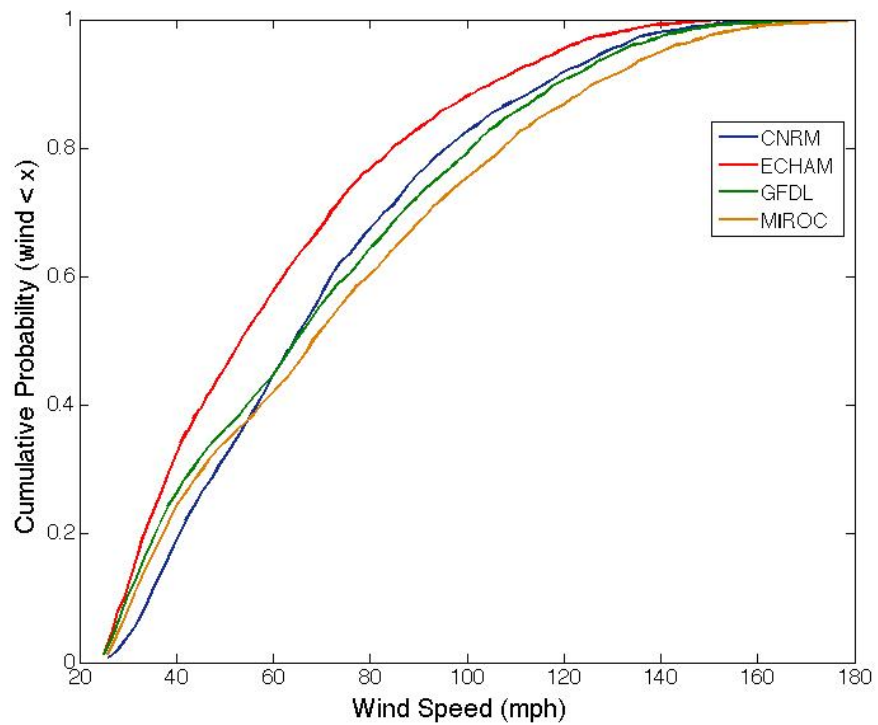
Figure 3. Maximum wind speed cumulative for 3000 storm arrivals at Galveston, for four AOGCMs under 2000 climate conditions, conditional on storm arrival.
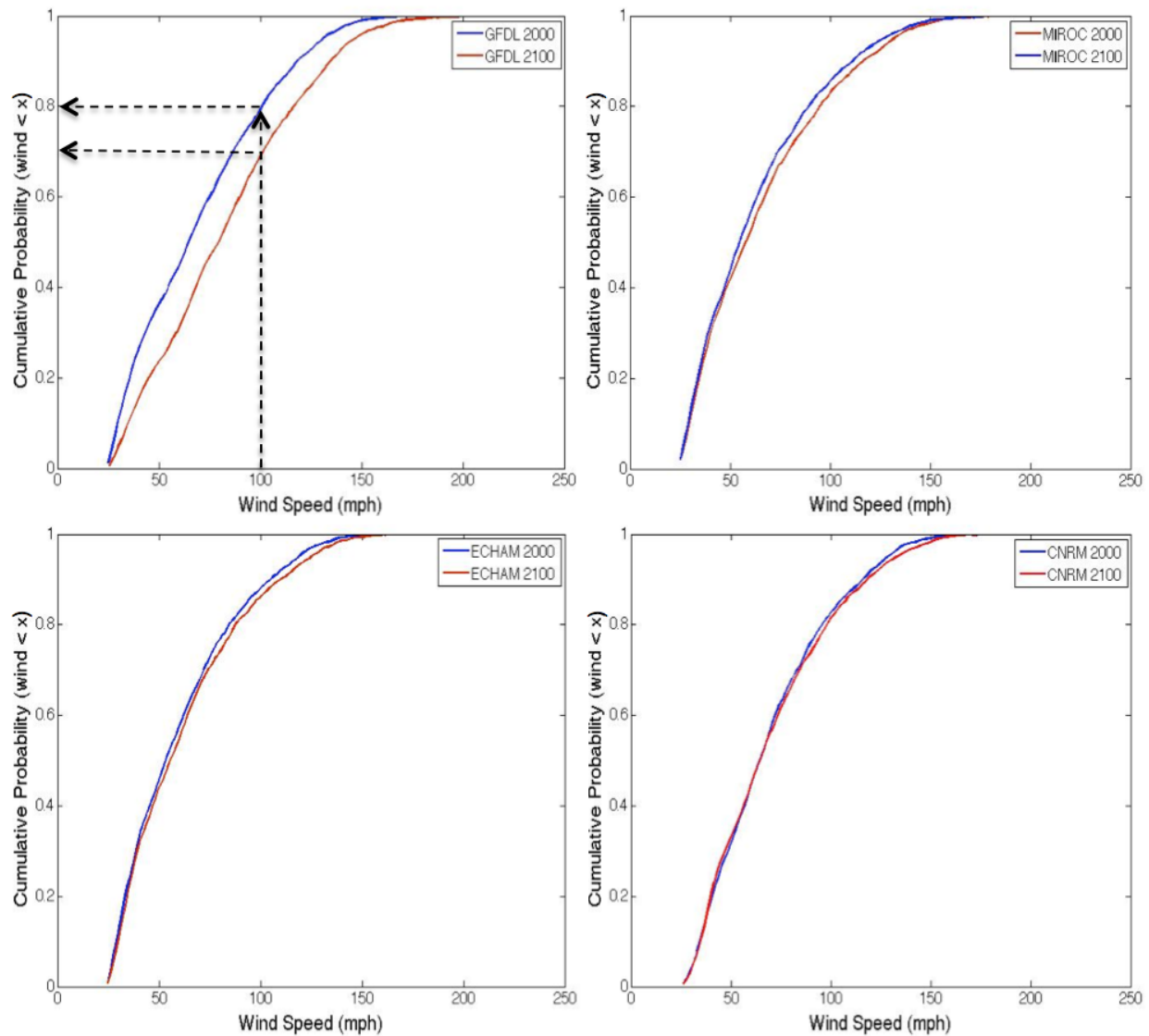
Figure 4. Cumulative distribution of maximum wind speed in Galveston Bay for the four GCMs used in the hurricane analysis. 2000 and 2100 probabilities are conditional on storm arrival.

8

Galveston Bay's surrounding coastline to generate corresponding surge events in the 2000 and 2100 climates. The storm surge heights used in this analysis are the maximum levels generated by SLOSH at the location closest to our facility of interest, which is 5 ft. above mean sea level (point A in Figure 1). Note that sea level rise is not included at this point in the analysis.

We can compare the differences in surge heights across climates by contrasting the probability density function in 2000 against that in 2100 in each model. These results are shown in **Figure 5**, and the analysis indicates that, for the GFDL model, the probability of an arriving surge exceeding 5 ft at Point A is projected to increase from 5% in 2000 to 7% in 2100. This change is smaller for the other three models used in our analysis. (Note again that these distributions of surge heights are conditional on storm arrival, and the risk does not yet include astronomical tide, sea level rise or subsidence.)
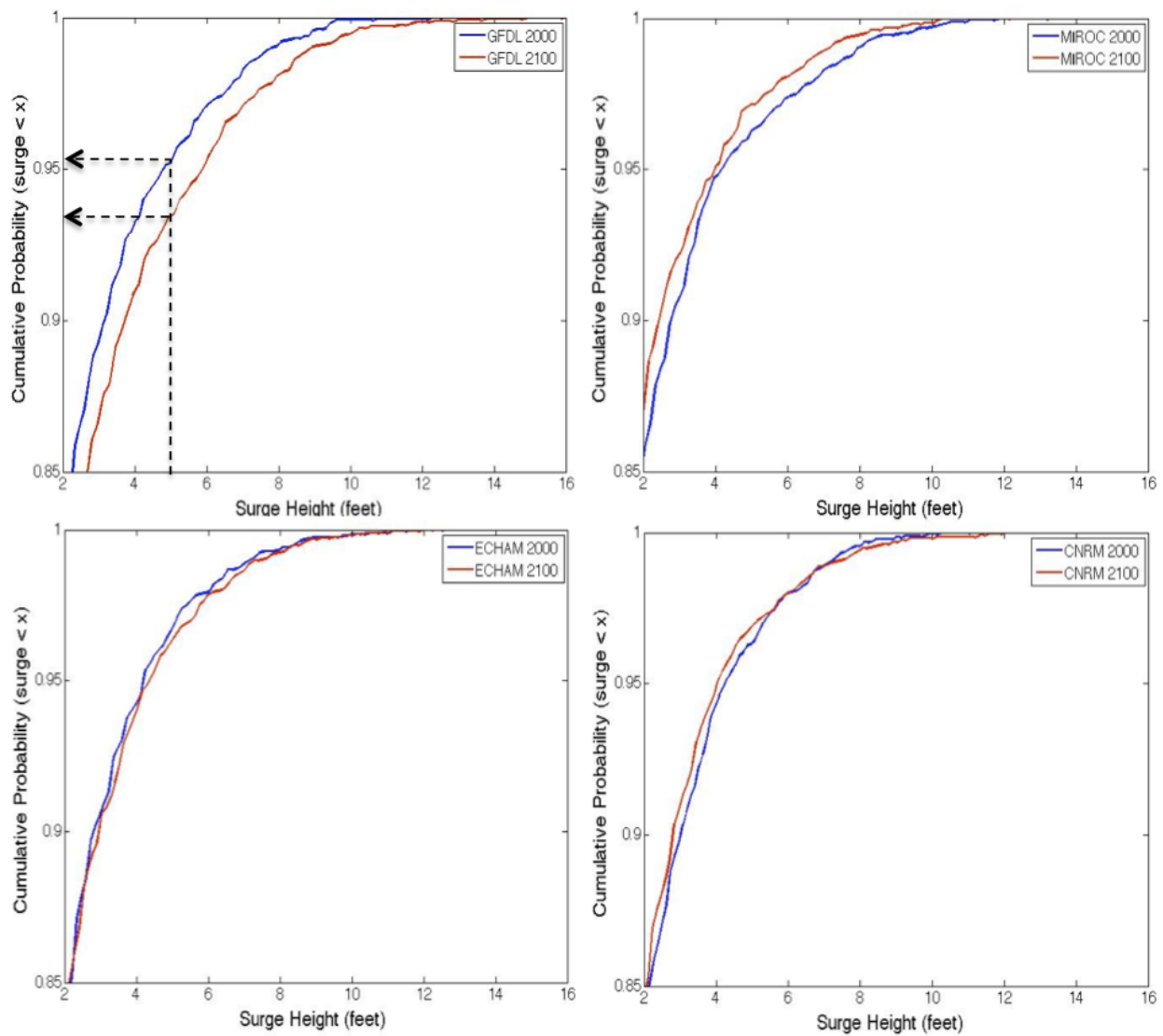
Figure 5. Cumulative distribution of maximum surge heights in Galveston Bay, 2000 and 2100 conditional on storm arrival.

3.1.3 Frequency and Probability of Surge

A number of conditions must exist for the seeds to develop into tropical storms. Hurricanes require pre-existing weather disturbances, atmospheric moisture, warm ocean water, and small vertical shear of prevailing winds. The degree to which these ideal conditions are met changes with a warming climate, and a different potential is reached for these seeds to develop into storms. Each climate model projects different conditions and so produces a different frequency of intense storms. These annual frequencies for each model's 2000 climate are calibrated to be in statistical agreement with the historical annual frequency. This same calibration coefficient is applied respectively to the 2100 climate of each model.

Also, an additional local calibration is performed using the historical storm frequency for the study site from the hurricane database, HURDAT, which is a historical record of Atlantic storms (Jarvinen and Lawrence, 1985). The HURDAT data set was updated in 2001 and again in 2002 to include reanalysis data for storm tracks as far back as 1851. In our analysis the annual frequency for the 2000 climate period in Galveston Bay, taken from HURDAT, is the observed number of tropical storms, above the specified minimum threshold of 34 mph, that pass through the filter in Figure 1 in a year. According to HURDAT, this frequency is 0.26, so the annual frequency for each model, under the 2000 climate, is set to this level, and the frequency for each model under the 2100 climate is then estimated based on the simulated frequency ratio (between the 2000 and 2100 climates). The estimated annual frequencies for ECHAM, GFDL, MIROC, and CNRM models are 0.28, 0.61, 0.29, and 0.28, respectively. Note that the GFDL model estimates a substantial increase in frequency relative to the other three models.

We assume that hurricane arrival times are independent of one another and therefore that they follow a Poisson distribution with annual frequency as the parameter.

The probability distributions of storm conditions in Figures 3 to 5 show the risk conditional on storm arrival. We seek, however, to find the distribution of the *annual* risk of flooding. Since this is a Poisson process, more than one storm could arrive in a year, but similarly there will be years with no storms. If more than one storm were to arrive in a year, we would only need to count the storm with the highest achieved surge height since any lesser storm's height would be exceeded by the most extreme.

To combine all processes, we use a numerical approximation to derive the resulting distribution from the Poisson storm arrival process. Define N_k as the number of storm arrivals in one year. We sample 100,000 times by first sampling the number of storms, N_k, from a Poisson distribution, then drawing N_k times from the distribution of storm surges given an arrival. We store the highest of the N_k storms for our yearly arrival height; if $N_k = 0$ then the highest surge height is stored at zero for that sample. The result is a new distribution, expressing the annual probability of surge heights, which we carry forward for the remainder of the analysis.

In this analysis, the astronomical tides in Galveston are approximately one foot, we linearly add tidal heights to surge heights by numerically drawing from a sinusoidal curve of magnitude one foot. In locations where tides are greater, their impacts on the height of a storm surge has the potential to be more significant. An incoming storm arriving at the same time as an incoming tide

usually contributes to a resulting water height less extreme than the linear combination of the tide and surge (e.g., Lin *et al.* (2012)). Therefore, using the linear combination is conservative in the sense that it assumes the less fortunate combination of events.

3.2 Sea Level Rise

The increasing risk from rising sea level is decomposed into thermal expansion plus flow from melting glaciers and ice caps (the better-understood component) and contributions from the continental ice sheets, especially the Greenland Ice Sheet (GIS) and the West Antarctic Ice Sheet (WAIS). For each contributor we include an analysis of uncertainty in change over the century. Considering the shortcomings of the underlying scientific understanding of the dynamics of the GIS and WAIS, our effort should be viewed less as a well-informed estimate and more as a demonstration of the type of analysis needed to support risk-based adaptation decisions.

3.2.1 Thermal Expansion Plus Glaciers and Ice Caps

There are six AOGCMs in the IPCC AR4 that include sea level projections in their results (**Table 3**). These sea level projections include thermal expansion as well as small contributions from glaciers and ice caps. (They also include a small addition from continental ice sheets, but not the dramatic effect that could occur if rising air and ocean temperatures accelerate the flow off the GIS and WAIS.) We perform a linear regression with the GCM results in Table 3, to derive an estimate of the relationship between temperature change and their estimate of sea level rise. Katsman *et al.* (2008) suggest that the relationship between thermal expansion and atmospheric temperature is linear and this assumption underlies the procedure. The estimate is based on the decade-averaged change in temperature between 2000 and 2100 and the decade averaged change in sea level between 2000 and 2100. The temperature change pathway is not included in the analysis; we assume the resulting change that is projected at the end of the century to be sufficient. We also assume that the residuals are normally distributed. For details see Lickley.

By this method the risk of thermal expansion follows a normal distribution with mean of $0.027T_i + 0.19$ where T_i is the decade averaged temperature change across the century, and the norm of the residuals implies a variance of 0.17367^2. The incorporation of this result in the overall risk analysis is discussed below.

3.2.2 Continental Ice Sheets

In the current century the main threat from loss of continental ice is from the GIS and the WAIS. Unfortunately, great uncertainty is attached to the behavior of these sources, presenting a severe challenge to the incorporation of this risk in an analysis of flood potential and adaptation decision. On the other hand, it would be misleading to ignore this component because some analyses project that the GIS and WAIS could contribute as much as 2 m of sea level by 2100.[3]

---

[3] Some studies of coastal risk incorporate a single scenario value of their contribution (e.g., Lin *et al.*, 2012) which gives an impression of the total risk but unfortunately involves the implicit assumption that the ice sheet contribution is certain at the scenario value applied.

Table 2. Global Circulation Model's from IPCC AR4. Temperature and sea level rise estimates based on A1B emissions scenario.

Model Name	Temperature Change	Sea Level Rise
CCMA CGCM 3.1	2.60 ^{o}C	0.210 m
GISS AOM	1.79 ^{o}C	0.343 m
GISS MODELE-R	1.75 ^{o}C	0.281 m
INMCM 3.0	2.16 ^{o}C	0.239 m
MIROC 3.2 (high res)	3.71 ^{o}C	0.338 m
MIROC 3.2 (med res)	3.10 ^{o}C	0.276 m
MRI CGCM- 2 3.2a	2.07 ^{o}C	0.134 m

Expert elicitation of ice and ocean analysts—e.g., of the type of applied to other climate variables by Morgan *et al.* (2006), and Morgan and Keith (1995)—could produce the type of uncertainty representation that is needed, but to date none has been published. Therefore, to complete the analysis of the Galveston Bay example, and to show how the needed information would be included in a decision framework we develop our own judgmental estimate of this aspect of changing flood risk.

Recent studies use a variety of approaches and show a wide range of estimates of sea level rise including the GIS and WAIS effects. Katsman *et al.* (2011) anticipate a high level scenario of 0.55 to 1.15 m in global mean sea level rise by 2100. This range is achieved by finding distributions for the high end contributions of each individual component. The medians of these distributions are then added together and their uncertainties are summed quadratically. Nicholls and Cazenave (2010) project a sea level increase of as much as 2 m, with an undefined but low probability. Vermeer and Rahmstorf (2009) project a rise in sea level between 0.97 and 1.56 m above 1990 levels by 2100 with a model average of 1.24 m. Nordhaus (2010), experimenting with an extension to the RICE model, anticipates that, under an emission trajectory similar to A1B, we will see a sea level rise of 0.73 m by 2100. His analysis considers the GIS and WAIS ice sheets individually, in an analysis that extends out several hundred years. The loss from the GIS starts with an estimate of its long-term ice volume under different temperature conditions and imposes a dynamic process of progression over time. WAIS is assumed to begin to melt only at 3 ^{o}C above current temperature and to discharge from that point at an increasing rate as temperature further rises. This procedure leads to a GIS contribution of 0.2 m and a very small release from the WAIS.

Some of these studies do not clearly distinguish the great ice sheets from other contributors to an overall sea level rise result, and they are based on different assumptions about the increase in global temperature over the period. Finally, most produce an estimate of global average sea level while the Katsman analysis tries to account for the rise at a particular point (the Netherlands). Taking these factors into account we represent the contribution of the continental ice sheets to sea level rise in Galveston Bay by a lognormal distribution with mean 0.6 m, and standard deviation of 0.14 m.

3.3 Subsidence

We approach this portion of the analysis again with wide uncertainty. The rate of subsidence will depend on several factors, including what is extracted from the ground (water, natural gas, oil). Thus the rate of subsidence can to some degree be altered by changes in policy and human activity. Given these unknown factors, predicting the rate of subsidence is a challenge. We base our estimate on the previous century's subsidence levels (**Figure 6**). The location of interest sits in a zone that has seen roughly between 3 and 4 feet of subsidence between 1906 and 2000. To estimate this coming century's subsidence, we use a triangular distribution. We assume that there will likely be a slower rate of subsidence given an increased understanding of the causes and potential developments in technologies to reduce subsidence. We therefore assume a mean of 2 feet and use 4 feet as our upper bound. We use zero for our lower bound and construct a triangular distribution on these three parameters.
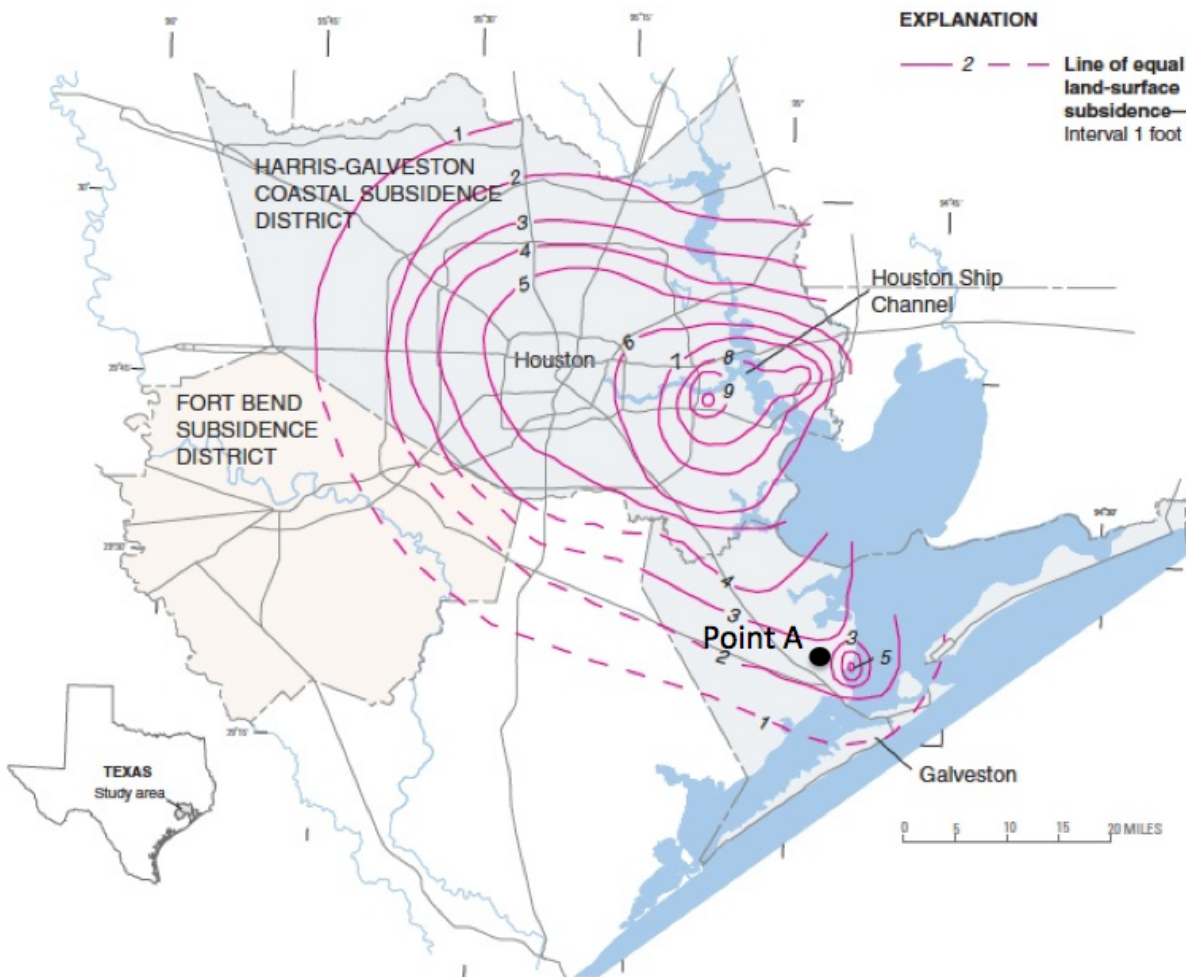
Figure 6. Contour map of Galveston subsidence regions between 1906 and 1987, (Source: Prince and Galloway (2001)).

Table 3. Probability of Flooding for facility at 5 feet in elevation.

Model Name	Annual Flood Risk (1980–2000	Annual Flood Risk (2080–2100)
CNRM-CM3	0.0099	0.5512
ECHAM	0.0093	0.5586
GFDL-CM2.0	0.0127	0.6150
MIROC 3.2	0.0108	0.5828

3.4 Annual Probability of Flood Events

To account for the combined impacts of all of these risks, we combine these four distributions. For present conditions sea level rise and subsidence are ignored and only storm arrivals under current intensities, frequencies and tides are considered. For the 2100 climate we use a numerical approximation by sequentially sampling from each of the distributions and adding the sampled sea heights (or sunken ground levels in the case of subsidence) together linearly. We repeat this Monte Carlo procedure 10,000 times for each climate to get an approximation of the combined risk distribution. The change in risk distribution across climates is shown in **Figure 7**. For the GFDL model and under our stated assumptions, the analysis concludes that, for a facility sitting at 5 feet at Point A in Figure 1, there is a 1.27% chance of flood heights reaching or exceeding that facilities elevation in one year under 2000 conditions and that this probability increases to 61.5% under 2100 conditions. See **Table 4** for the results from all four models.

4. ECONOMIC ADAPTATION TO RISING RISK

4.1 A Dynamic Programming Formulation

We assume that adaptation of the facility at Point A to this increased risk of coastal flooding will involve the construction and maintenance of levees[4], and that at any time the option will be available to build a levee or add to an existing one. As risks increase over time, there will come a growing need for adaptation or abandonment, and this decision depends on both the then current flood risk and the expected future risk. For example, a refinery at the water's edge facing a rising flood risk faces decisions about whether to keep the facility or abandon the site and, if it is to be kept, the degree of protection to add now, say by raising a levee. These choices depend on the value of the facility, on the cost of different levels of protection and the damage that it might prevented over time, and on the possibility that it can be augmented later. It is a dynamic programming problem that takes account of the influence of current and future conditions on todays choice.

During each time period, we consider the state of the facility and all possible decisions available within that state. The state is the level of protection in place (the height of the levee in feet), and the decision options consist of the number of additional feet to build, including the

---

[4] Levees do have the potential to fail, as observed in New Orleans during Hurricane Katrina. In this analysis we assume no failure and further assume that once a levee is constructed, it is maintained through time.
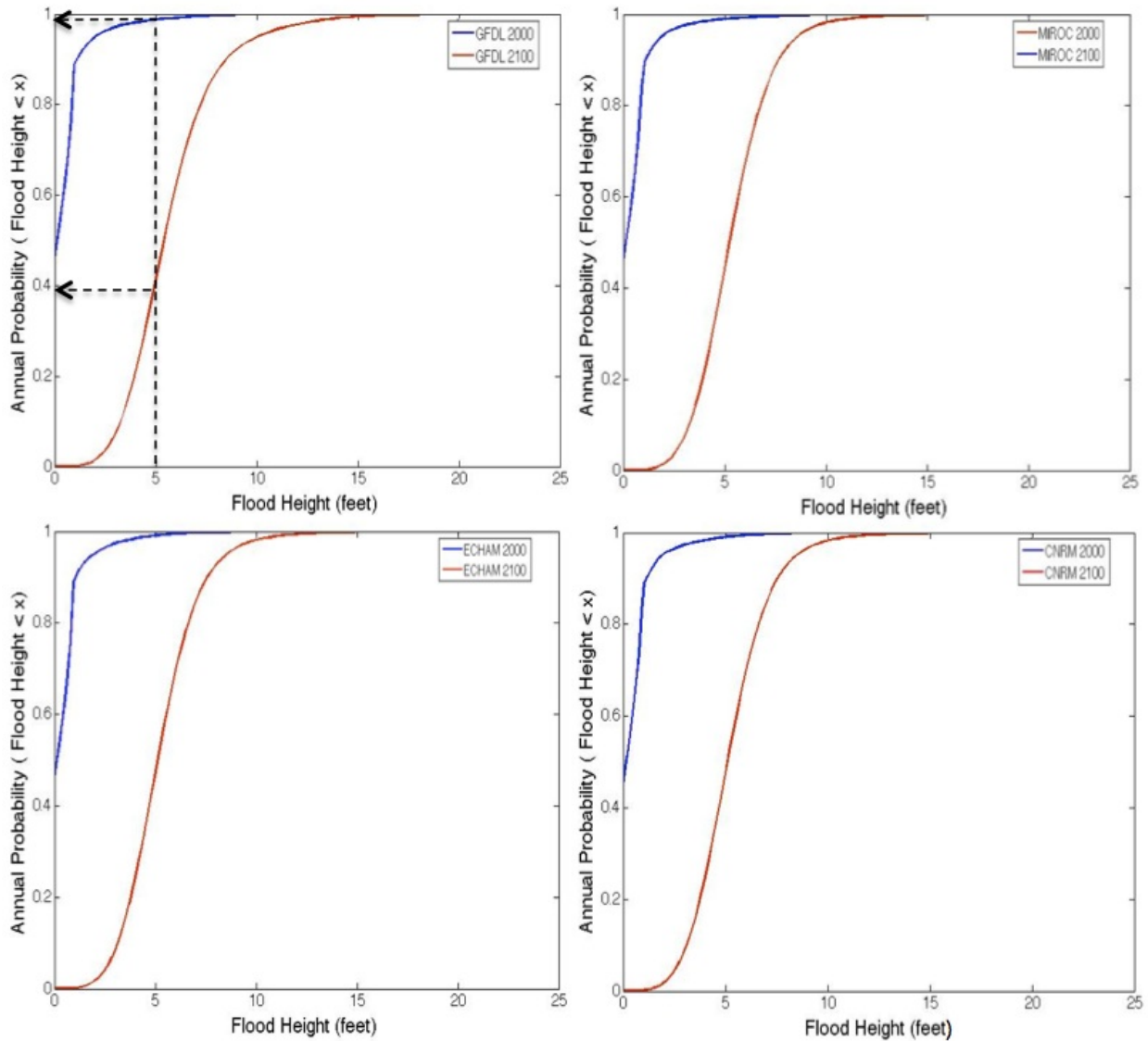
Figure 7. Change in annual risk of inundation including risks of storm surge (included here is the change in frequency across climates), thermal expansion, sea level contributions from WAIS and GIS, and subsidence. The blue line is the probability distribution of inundation in 2000 and the red line is the probability distribution of inundation in 2100.

15

option to do nothing. The expected loss at any point in time is a function of current as well as future states and actions. The procedure begins by optimizing in the last period and working back toward the present. To limit the decision options we only consider adaptation options between 2000 and 2100 and we allow decisions for additional structures to be made at each decade (this means that the last state under consideration for decision making is the 2090–2100). Further, we allow for up to a 20 foot levee to be added on in 2 foot increments.

Define S_t to be the state and $A_t(S_t)$ to be the best action respectively during decade t, yielding the lowest expected costs at decade t in state S_t. Further, let $C_t(S_t, A_t)$ be the expected costs during decade t given state S_t and action A_t. For each time period, we calculate the best action and lowest value such that

$$A_t(S_t) = \arg\min_{A_t} \left\{ C_t(S_t, A_t) + \frac{1}{(1+r)^{10}} V_{t+1}(S_t + A_t) \right\}, \tag{1}$$

and

$$V_t(S_t) = \min_{A_t} \left\{ C_t(S_t, A_t) + \frac{1}{(1+r)^{10}} V_{t+1}(S_t + A_t) \right\}, \tag{2}$$

where r is the discount rate. $C_t(S_t, A_t)$ is defined as:

$$C_t(S_t, A_t) = E(Damage|S_t, A_t) + c_m \times m \times S_t + c_b \times m \times A_t, \tag{3}$$

where $E(Damage|S_t, A_t)$ is the expected damage during the decadal time period given the state and action made at the beginning of that time period, c_m is the cost of maintaining one foot-mile of sea wall, c_b is the cost of building an additional foot-mile of sea wall, $V_t(S_t)$ is the value of expected current and future costs discounted to decade t, and m is the number of miles of sea wall necessary to protect the facility. Since we choose to look at decisions made every decade, each of these costs are accumulated over the decade, with the discount rate of r.

We obtain probabilities of yearly inundation by interpolating between the two probability distributions for each of the models in Figure 7. **Figure 8** shows the interpolated risk profiles for GFDL. We interpolate the flood heights linearly between percentiles. For instance, if the 60th percentile of flood heights is 0.5 feet in 2000 and 5.5 feet in 2100, then the 60th percentile for the intermediate decades will be 1 foot in 2010, 1.5 feet in 2020, 2 feet in 2030 and so on. For the other components of the risk analysis (i.e. dynamic great ice sheet loss, subsidence and hurricane intensity), there is a lack of scientific understanding of how the ice loss will progress over the century. Due to the weak scientific basis, our default assumption is a linear trend in a changing risk profile. Future work is needed to develop simulations for the intermediate decades between 2000 and 2100.

From these probability distributions, we can find $P_t(\zeta > \xi + S_t + A_t)$, which is the probability that the flood height, ζ, will exceed the wall height at elevation ξ in a given year with a protection height of $S_t + A_t$. To derive the expected damages over the tth decade, we calculate the sum of

16
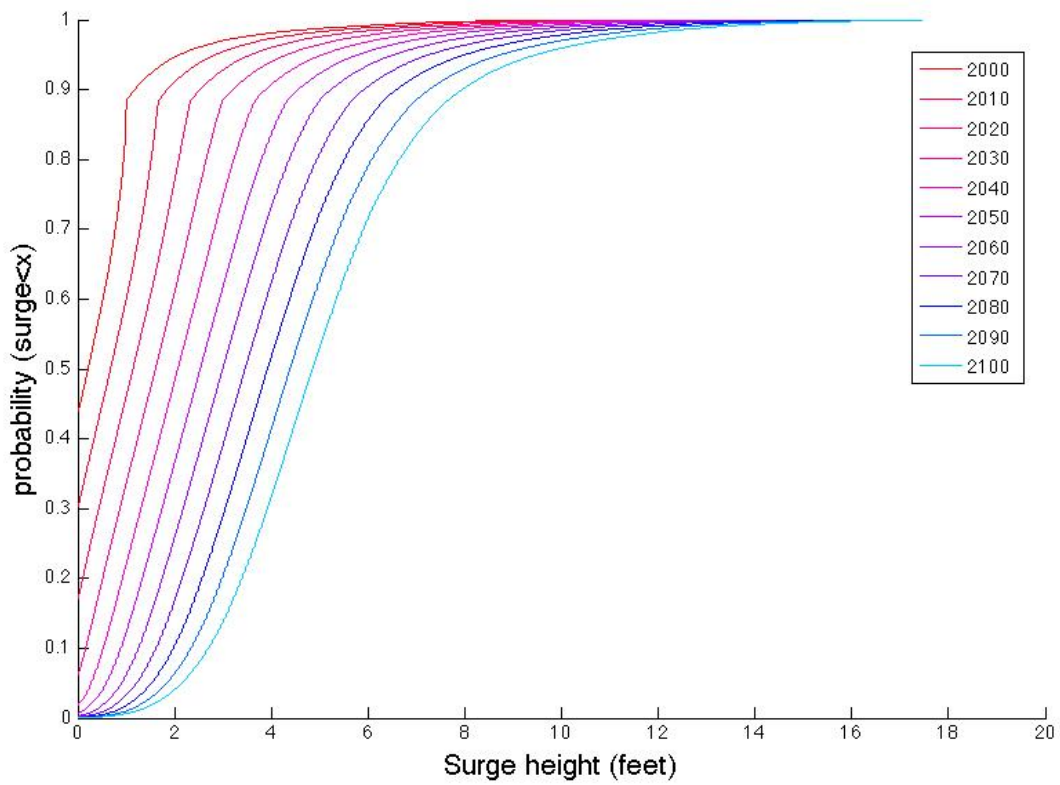
Figure 8. Interpolated GFDL model risk profiles for each decade.

expected damages for each year:

$$E(Damage|S_t, A_t) = \sum_{i=1}^{10} \frac{1}{(1+r)^{i-1}} \times D \times P_t(\zeta > \xi + S_t + A_t),\tag{4}$$

where D is the damage incurred by a flooded facility and i is a year in decade t. By iterating backwards over time, we are able to derive the optimal wall height for each state.

4.2 The Current Decision to Protect

We illustrate this method using a case of a flooded facility of similar magnitude to facilities that exist at 5 feet above today's mean sea level in Galveston. The flood-related costs incurred by this facility include the sum of lost or damaged infrastructure, loss of operational capacity until repairs were finished, and any legal costs for damaged third-party property. Data is not available on potential damage to the refinery actually located at our point of interest in Galveston Bay, so to illustrate the method we construct a case of a 200,000 barrel per day refinery at that point and apply estimates loosely based on a facility flooded by hurricane Katrina. The resulting model parameters are the following:

- $D = \$650 million$ Expected cost of flood event
- $c_m = \$4330$ Maintenance cost per foot-mile of levee
- $c_b = \$1,000,000$ Capital cost per foot-mile of levee
- $m = 5$ miles   Length of levee required
- $r = 0.05$ Interest rate
- $\xi = 5$ ft.   Height of facility above mean sea level

The result is the decision-making sequence that yields the minimum expected cost, flood damage plus protection. Note that this decision sequence is based on current perceived climate risks and will change as understanding of the risks changes over time. Under these parameters, the sequence of decisions for levee height with this model is outlined in **Figure 9**. Each climate model leads to a different sequence of heights with the GFDL model indicating the highest level of protection over time. CNRM and ECHAM produce an identical protection sequence, beginning with 4 feet of protection for the first decade.

This decision-making framework also can be used to inform abandonment decisions. The associated costs with the GFDL sequence are $52.7 million. If today's net present value of the facility were lower than this amount, then the expected damages would outweigh the benefits of keeping the facility in operation and the economic response would be to abandon the facility.

We apply this framework to a risk profile that remains constant over time, i.e. assuming no change in sea level or hurricane activity over time and no additional subsidence. The results show that the economic level of protection with no expectation of changing climate and continuing subsidence would be a 6 foot levee for both MIROC and GFDL, and 4 feet for ECHAM and CNRM.
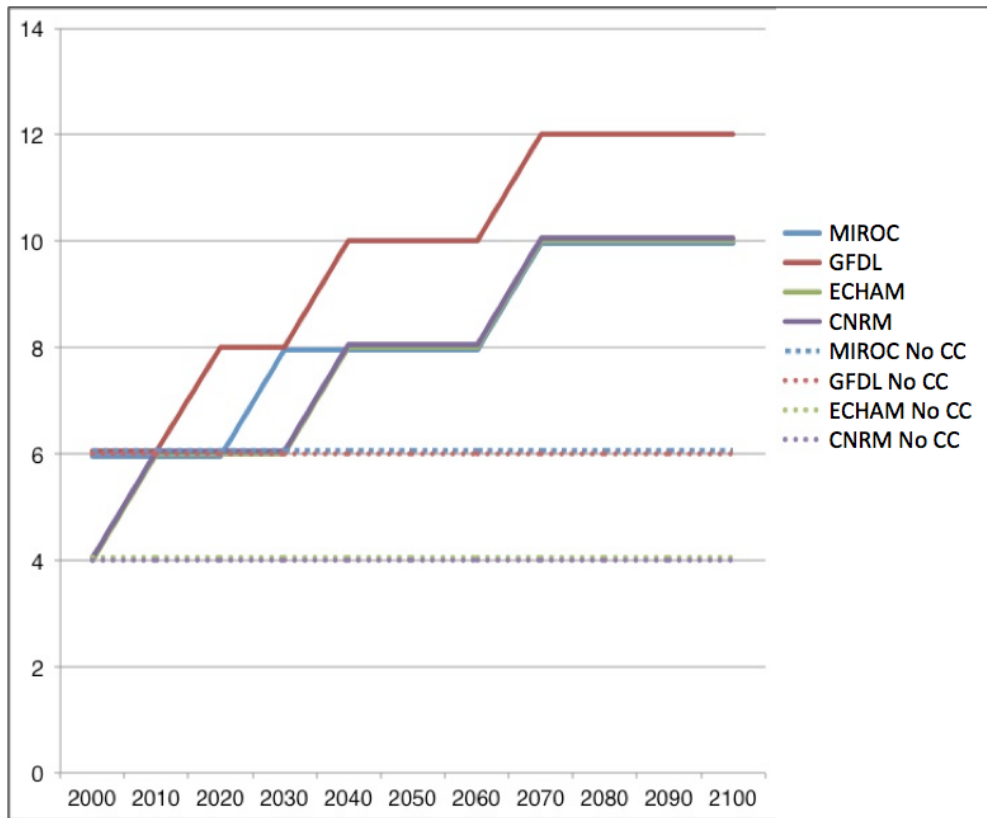
Figure 9. Optimal levee height (in feet) across decades generated by each AOGCM. The 'No CC' horizontal dotted lines are the optimal levee heights determined from each model under a future scenario with no climate change.

This framework also can illuminate situations where the economic decision might be viewed as infeasible at present. If a levee is thought unaffordable today or if regulations restrict the construction now, the analysis can estimate the cost of delay. For instance, if a sea wall can't be constructed in 2000 but is feasible in 2020, then the expected accumulated costs in 2020 will be $50 million. The total expected costs in 2000 would also need to include the expected costs of no protection for the first two decades. Using risk profiles for 2000 and 2010 the extra expected costs of leaving a facility unprotected during this period are an additional $148 million in expected damages incurred in that time frame, which could serve as a justification for relaxing financial constraints or changing regulations.

5. STEPS TO PRACTICAL APPLICATION

With the Galveston Bay example we demonstrate how analysis of changing coastal risk may be brought to useful application to decisions about adaptation. However, this sample application highlights the additional research and analysis needed to increase the usefulness of this approach to decision support. Some issues are well within the method applied here. Additional climate science research would include the calculation of one or more intermediate time steps in the storm and surge analysis, to inform the evolution of risk over time as displayed in **Figure 8**. Also, a more detailed surge model like ADCIRC could be applied. Additional economic analysis could make provision for economies In the economic of scale in protection investment, and could take account of the probability of levee failure. Current damage is considered to be equal for all flood levels. Variations in damage costs could be included for varying flood levels.

Other potential improvements require more fundamental research. Of particular importance is the need for probabilistic analysis of the contribution of the continental ice sheets to sea level rise. Understanding of the dynamics of these ice sheets is poor, and knowledgeable scientists are understandably reluctant to put forward estimates of the likelihood of different levels of contribution— Analyses predict only a range— sea level shold rise more than X feet and may rise as much as Y feet. For decision support in the face of the combination of coastal risks more is needed, and in the absence of credible ice models, a process of expert elicitation of scientists engaged in the work would be superior to high and low scenarios containing no notion of likelihood.

A further limitation of this and other efforts on coastal risk is that the risk results frequently are conditioned on so many assumptions. The analysis above is typical. First, it is conditional on the A1B emissions scenario, whereas there is considerable uncertainty regarding future emissions growth. Secondly, the result is conditioned on single runs of particular models. Some notion of the uncertainty in climate projection can be seen in the differences among the models used here (see Table 3). Unfortunately, this comparison among single runs of AOGCMs only partially accounts for the uncertainty in climate projection. Such studies have been done with earth models of intermediate complexity (e.g., Sokolov *et al.*), but those models do not represent the climate system with the complexity needed to support the track and intensity analysis developed by Emanuel *et al.* (2006) and Emanuel *et al.* (2008) and applied here. Therefore an important research task is to seek ways to introduce uncertainty analysis into the variables input to the storm

simulations.

If, however, some of these analysis problems can be alleviated, this approach can serve a number of emerging problems in the analysis of coastal risk and the timing and scale of adaptation measures. The estimation of the coming change in physical flood risk, even if conditioned on a number of assumptions as above, will be useful in anticipating the changes that may be required in the FEMA flood mapping system and the flood insurance programs that are tied to it. City, state and regional authorities faced with issues of zoning, building standards and efforts to anticipate future investment in protection would need analysis of this type to inform both magnitude and timing of actions. A productive avenue for next steps in research in this area, beyond the improvements in the analysis itself, is study of how such an effort might be structured, staffed and supported.

Analysis of this type is available from consulting firms, for the private companies and government agencies that can afford to pay for it, but a more generally available source of analysis and insight is needed for the broader national challenge of dealing intelligently with the rising risk.

Acknowledgements

6. REFERENCES

Deser, C., R. Knutti, S. Solomon and A. Phillips: Uncertainty in the Backyard: Communicating the Role of Natural Variability in Future North American Climate. *Nature Climate Change*, **2**(1562): 775–779.

Emanuel, K., 2005: Increasing destructiveness of tropical cyclones over the past 30 years. *Nature*, **436**(7051): 686–688.

Emanuel, K., C. DesAutels, C. Holloway and R. Korty, 2004: Environmental control of tropical cyclone intensity. *Atmospheric Science*, **61**: 843–858.

Emanuel, K., S. Ravela, E. Vivant and C. Risi, 2006: A statistical deterministic approach to hurricane risk assessment. *Bulletin of the American Meteorological Society*, **87**(3): 299–314.

Emanuel, K., R. Sundararajan and J. Williams, 2008: Hurricanes and global warming. *Bull. Am. Meteorol. Soc*, **89**: 347–367.

FEMA: Guidelines and Specifications for Flood Hazard Mapping Partners, Appendix D: Guidance for Coastal Flooding Analyses and Mapping. *Federal Emergency Management Agency*: Washington, DC.

Galloway, D., D. Jones and S. Ingebritsen, 1999: *Land subsidence in the United States*. US Geological Survey.

Jarvinen, B. and M. Lawrence, 1985: Evaluation of the SLOSH Storm-Surge Model. *American Meteorological Society Bulletin*, **66**(11).

Jelesnianski, C., J. Chen and W. Shaffer, 1992: *SLOSH: Sea, lake, and overland surges from hurricanes*. US Department of Commerce, National Oceanic and Atmospheric Administration, National Weather Service.

Katsman, C., W. Hazeleger, S. Drijfhout, G. Jan van Oldenborgh and G. Burgers, 2008: Climate scenarios of sea level rise for the northeast Atlantic Ocean: a study including the effects of ocean dynamics and gravity changes induced by ice melt. *Climatic Change*.

Katsman, C., A. Sterl, J. Beersma, H. van den Brink, J. Church, W. Hazeleger, R. Kopp, D. Kroon, J. Kwadijk, R. Lammersen *et al.*, 2011: Exploring high-end scenarios for local sea level rise to develop flood protection strategies for a low-lying deltathe Netherlands as an example. *Climatic change*, **109**(3): 617–645.

Lickley, M.: *The Vulnerability of U.S. Coastal Energy Infrastructure Under Climate Change.* Master of Science Thesis in Technology and Policy, Augest.

Lin, N., K. Emanuel, J. Smith and E. Vanmarcke, 2010: Risk assessment of hurricane storm surge for New York City. *Journal of Geophysical Research*, **115**(D18): D18121.

Lin, N., K. Emanuel, M. Oppenheimer and E. Vanmarcke, 2012: Physically based assessment of hurricane surge threat under climate change. *Nature Climate Change*, **2**(1389). doi:10.1038/NCLIMATE1389.

Meehl, G. A., C. Covery, T. Delworth, M. Latif, B. McAvaney, J. F. B. Mitchell, R. J. Stouffer and K. E. Taylor, 2007: The WCRP CMIP3 multi-model dataset: A new era in climate change research. *Bulletin of the American Meteorological Society*.

Morgan, M. and D. Keith, 1995: Subjective Judgments by Climate Experts. *Environmental Science Technology*, **29**(10): 468A–476A. doi:10.1021/es00010a753.

Morgan, M., P. Adams and D. Keith, 2006: Elicitation of expert judgments of aerosol forcing. *Climatic Change*, **75**(1): 195–214.

Nicholls, R. and A. Cazenave, 2010: Sea-level rise and its impact on coastal zones. *Science*, **328**(5985): 1517–1520.

NOAA: [US National Oceanic and Atmospheric Adminstration], Hurricane Basics. *U.S. Department of Commerce*: Washington D.C.

Nordhaus, W., 2010: Projections of Sea Level Rise (SLR). *unpublished*.

Prince, K. and D. Galloway, 2001: U.S. Geological Survey Subsidence Interest Group Conference, Proceedings of the Technical Meeting, Galveston, Texas, November 27–29. *U.S. Geological Survey*.

Sokolov, P., P. Stone, C. Forest, R. Prinn, M. Sarofim, M. Webster, S. Paltsev and C. Schlosser: Probabilistic forecast for twenty-first-century climate based on uncertainties in emissions (without policy) and climate parameters. *Climate*, **22**: 5175–5204. doi:http://dx.doi.org/10.1175/2009JCLI2863.1.

Solomon, S., D. Qin, M. Manning, Z. Chen, M. Marquis, K. Averyt, M. Tignor and H. Miller, 2007: Climate Change 2007: The Physical Science Basis. *International Panel on Climate Change*, **Fourth Assessment Report**.

Vermeer, M. and S. Rahmstorf, 2009: Global sea level linked to global temperature. *Proceedings of the National Academy of Sciences*, **106**(51): 21527–21532.

Yergin, D., 2006: Ensuring energy security. *Foreign Affairs*, **85**(2): 69–82.

REPORT SERIES of the MIT Joint Program on the Science and Policy of Global Change

Contact the Joint Program Office to request a copy. The Report Series is distributed at no charge.